VOL. 11, NO. 24, DECEMBER 2016 ISSN 1819-6608
ARPN Journal of Engineering and Applied Sciences

www.arpnjournals.com

COMPUTATIONAL MODELING OF BRITTLE FRACTURE UNDER DYNAMIC LOADING

Sergey A. Zelepugin[1,2], Alexey S. Zelepugin[1,2] and Yuri F. Khristenko[1]
[1]National Research Tomsk State University, Tomsk, Russia
[2]Tomsk Scientific Center, Siberian Branch RAS, Tomsk, Russia
E-Mail: szel@yandex.ru

ABSTRACT

This paper presents a fracture model of brittle materials subjected to high velocity impact. The verification of the model is carried out by comparing computational results with the data obtained from shock compression tests. The model is used to simulate the deformation and fracture of Al_3Ti - Ti metallic-intermetallic laminate composite under dynamic loading.

Keywords: brittle solids, intermetallics, strength of materials, model of brittle fracture, shock-waves.

INTRODUCTION

The wide use of composite materials in the constructions designed for operation under dynamic loads causes a steady interest in the study of their properties [1, 2]. Most of the composites include ceramic materials, so the experimental and theoretical investigations are intensively conducted to study the behavior of ceramic materials under dynamic loading [3-6]. In the computational investigation the most important stage in the developing and studying the behavior of structural elements is the application of an adequate material model. It concerns especially the ceramic materials exposed to shock-wave loading due to a difference in strength properties of such materials compared to metals and a substantial dependence of their properties on the microstructure of the material.

The possibility of the ceramics fracture during the process of shock-wave compression is an important question. The experimental data obtained [7, 8] show the various behavior of different ceramics during shock-wave compression. Boron carbide B_4C demonstrates all the signs of brittle fracture, including the increase in the average specific volume due to the formation of a large number of cracks (dilatancy). Silicon carbide SiC, on the other hand, in these conditions is plastically deformed, that is confirmed, among other things, by the fact that its spall strength remains relatively high during shock-wave compression above the Hugoniot elastic limit. The behavior of ceramic materials on the basis of aluminum oxide (Al_2O_3), aluminum nitride (AlN), titanium diboride (TiB_2), and zirconium dioxide (ZrO_2) is intermediate and combines plastic and brittle deformation mechanisms. In the majority of cases, the values for the spall strength of ceramics are within 0.5 - 1 GPa, and this value often drops to zero, or at least significantly decreases within the range of elastic limit.

At present a metallic-intermetallic laminate (MIL) composite is considered to be a new, promising, light and hard material [9, 10]. The superior specific properties of these composites make them attractive for high-performance aerospace applications, and the production method for creating MIL composites allows new embedded technologies to be incorporated into the materials, enhancing their functionality and utility [10]. The development of the technologies for the production of such materials, the laboratory test methods and the computational modeling of mechanical behavior under dynamic loading are of interest to modern materials science.

The Ti-Al_3Ti biomimetic multilayered composites were produced on the basis of layered microstructural composition found in mollusk shells [10]. This process is conducted in the open air in one stage and allows a nonporous laminate composite to be produced. A simple hot press is used as an installation for the production of the composite.

Before conducting the synthesis, the titanium and aluminum foils are combined, and the foil thickness is selected to provide complete consumption of the aluminum layer during the reaction with the adjacent layers of titanium. This arrangement of initial layers results in a composite with alternating layers of synthesized titanium aluminide Al_3Ti (similar to solid layers in shells, quite hard, but brittle) and residual titanium (plastic layer). The thickness of composite layers depends on the initial thickness of the aluminum and titanium foils.

High fracture resistance of MIL composites is due to the substantially anisotropic structure of the multilayered composite and the necessity of the crack to be initiated in each intermetallic layer. These composites can be used to perform various functions such as the thermal management (electrical conductors in ceramic isolators are embedded in composite panels before the synthesis), the damping of shock waves (using cavities built into the composite), the control through the built-in sensors, and as the ballistic protection [10].

The behavior of MIL composites under dynamic loading is of current interest. At present, there are a few of experimental works in the scientific literature devoted to studying the behavior of these composites under dynamic loading [10-12]. The experimental data show that it is not possible to identify the sequence, duration and contribution of different failure mechanisms to the development of damage areas in a composite target. Therefore, to analyze the behavior of MIL composites, the

ARPN Journal of Engineering and Applied Sciences

use of computational modeling becomes more important, since it allows the high-velocity loading of composite targets to be investigated in a wide range of initial conditions in the framework of an unified mathematical approach [12, 13]. The commercial code ANSYS is used in the computational modeling of the behavior of multilayered metallic-intermetallic composites [14]. However the intermetallic fracture models under dynamic loading has not been developed yet.

MODEL OF BRITTLE FRACTURE

In this work, a wide-range model is proposed to describe the brittle fracture of materials (ceramics, intermetallics, glass) at relatively low loading velocities (the velocity is about several hundred m/s) and sufficiently high loading velocities (about several thousand m/s). The model considers the possibility of the material fracture after exceeding the Hugoniot elastic limit in the shock wave, as well as the strength material characteristics (dynamic yield point) versus the achieved level of damage.

Unlike metals, the failure of which occurs under tensile loading, the modeling of brittle fracture requires considering both stages of loading such as compression and tension.

In this work the dependence of the dynamic yield point for modeling of the brittle material fracture during compression is given by:

$$\sigma = \begin{cases} \sigma_0, & \text{if } \sigma_z \geq P_{fr} \\ K_f \sigma_0, & \text{if } \sigma_z < P_{fr} \end{cases} \tag{1}$$

Here σ_z is the stress component in the shock wave ($\sigma_z < 0$ for compression); P_{fr} is the material constant ($P_{fr} < 0$). The coefficient K_f can be varied from 0 to 1. When $K_f = 0$, the dynamic yield point in the shock wave drops to zero after exceeding the Hugoniot elastic limit, which is typical for completely brittle fracture (for example, boron carbide), when $K_f = 1$ the character of deformation is completely plastic, and the dynamic yield point in the shock wave is not changed during compression. The intermediate values K_f allow the combined plastic deformation and brittle fracture to be described.

Under tensile loading, the dependence of the dynamic yield point in the modeling of brittle fracture is given by:

$$\sigma = \begin{cases} \sigma_0 \left(1 - \frac{V_f}{V_4}\right), & \text{if } V_f < V_f^k \\ \sigma_f, & \text{if } V_f^k \leq V_f < V_4 \\ 0, & \text{if } V_f \geq V_4 \end{cases}, \tag{2}$$

where V_f is the specific volume of microdamages (cracks) defined by the spall fracture model [8], V_4, V_f^k, σ_f are the constants.

For comparison, the dynamic yield point versus the damage level in the modeling of the behavior of plastically deformable materials is as follows [8]:

$$\sigma = \begin{cases} \sigma_0 \left(1 - \frac{V_f}{V_4}\right), & \text{if } V_f < V_4 \\ 0, & \text{if } V_f \geq V_4 \end{cases}. \tag{3}$$

The dynamic yield point versus the specific volume of microdamages for plastic (3) and brittle (2) materials under tensile loading is shown in Figure-1a and Figure-1b, respectively.

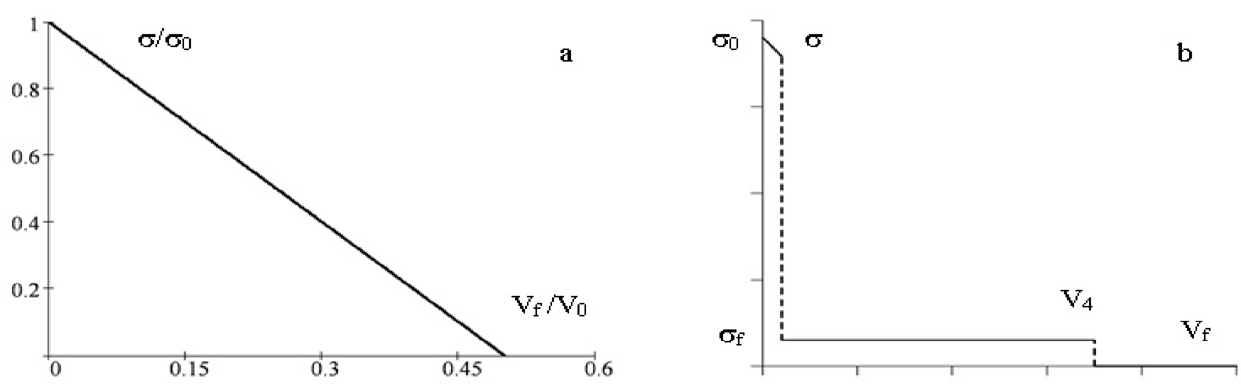

Figure-1. Typical dynamic yield stress versus the specific volume of microdamages for plastic (a) and for brittle (b) material.

VERIFICATION OF THE MODEL

Verification of the model was carried out by comparing with the experimental data obtained in the Sandia National Laboratories [3, 15]. The installation that produced a plane loading front in the sample for the specified time interval of the process was used in the experiments. The projectile was a ceramic plate made of a material identical to the material of the target. The projectile was accelerated by a gunpowder (89 mm internal diameter) or a two-stage light gas installation at velocities providing the peak pressure in the sample from 3 to 70 GPa (0.4 - 2.4 km/s for the gunpowder installation

VOL. 11, NO. 24, DECEMBER 2016 ISSN 1819-6608
ARPN Journal of Engineering and Applied Sciences

and higher for the light gas installation). The ceramic projectile velocity was measured using three electric sensors (velocity pins).

Four similar sensors (flush pins) controlled the plane of impact, and the deviation was usually less than 10^{-3} radians. The lithium fluoride window (LiF) was attached to the rear surface of the ceramic target by using epoxide resin with a layer sickness of 10 - 20 microns for observations with the use of a laser interferometer. The laser interferometer recorded the rear surface velocity of the ceramic sample through the window versus time of the process, including both the increase in the velocity of the rear surface due to the arrival of a compression wave and the decrease in the velocity due to the arrival of the unloading wave from the rear surface of the projectile.

The interaction of the projectile (ceramic plate 5 mm in thickness, 87.5 mm in diameter, the area D_1 in Figure-2a) with the sample (ceramic plate 10 mm in thickness, 76.2 mm in diameter, the area D_2) was numerically investigated for comparison with the experimental data. The window of lithium fluoride located behind the sample and occupying the area D_3 was 25.4 mm in sickness and 50.8 mm in diameter.

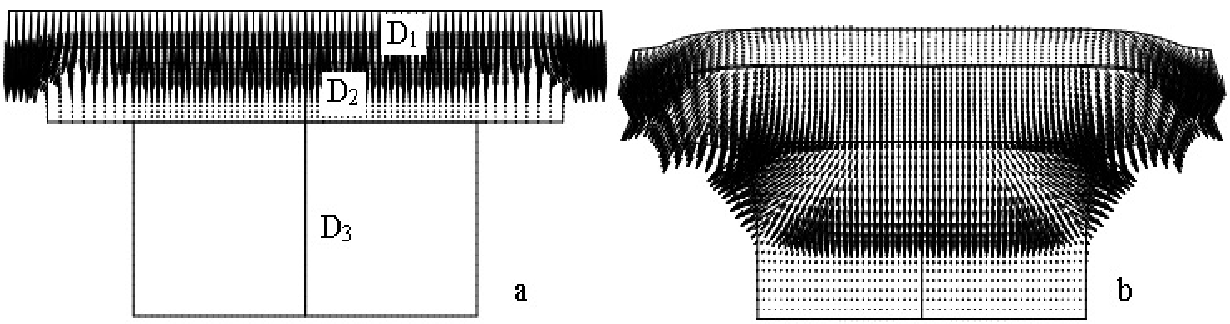

Figure-2. Computed configurations of the AD995 ceramic projectile (D_1) - AD995 ceramic plate (D_2) - LiF window (D_3) assembly and the velocity fields at the time of 0.5 (a) and 3.5 μs (b).

The numerical computations were carried out using the research computer code based on the modified finite element method without construction of the global stiffness matrix [16, 17]. For modeling of high velocity impact loading, a model of a damaged medium characterized by the presence of microcavities (pores or cracks) is used. The total volume of the medium comprises the undamaged part and microcavities of zero density. The damage level of the medium is characterized by the specific volume of pores V_f. The system of equations governing the nonstationary, adiabatic (for both elastic and plastic deformations) motion of a compressible medium with allowance for the evolution of microdamages comprises the continuity equation, the equation of motion, the energy equation [17].

Pressure in the undamaged substance is a function of specific volume of the undamaged substance and specific internal energy, and over the entire range of loading conditions it is determined by the Mi-Grüneisen equation of state. The constitutive relations connect the components of the stress deviator and strain rate tensor, and include the Jaumann derivative. The von Mises yield criterion is used. The critical value of the specific energy of shear deformations is used as a criterion of erosive material damage. The sliding boundary conditions are imposed to the contact surfaces between the projectile and the sample, as well as between the sample and the window of lithium fluoride.

The material constants used in the computations are given in Table [15, 18]. In Table ρ_0 is the density, c_l is the longitudinal sound velocity, G_0 is the shear modulus, σ_0 is the dynamic yield point.

Table-1. The constants of materials.

	ρ_0, kg/m^3	c_l, m/s	G_0, GPa	σ_0, GPa	σ_p, GPa	K_f	V_f^k, m^3/kg	P_{fr}, GPa	V_4, m^3/kg
AD995	3890	10560	160	4.7	0.3	0.4	$1.0 \cdot 10^{-5}$	-8.8	$1.75 \cdot 10^{-4}$
LiF	2640	5150	49	0.2	0.02	0.2	$1.0 \cdot 10^{-5}$	-2.4	$1.89 \cdot 10^{-4}$
Al_3Ti	3290	5122	83	1.6	0	0	$1.0 \cdot 10^{-5}$	-3.2	$1.22 \cdot 10^{-4}$
Ti	4426	4990	41	1.2	-	-	-	-	$1.35 \cdot 10^{-4}$
93W-7FeCo	18040	3692	77.5	3.0	-	-	-	-	$2.2 \cdot 10^{-2}$

VOL. 11, NO. 24, DECEMBER 2016 ISSN 1819-6608
ARPN Journal of Engineering and Applied Sciences

Figure-2 shows the computed configurations of the test assembly (for AD995 ceramics) and the velocity fields at the time of 0.5 and 3.5 μs at the initial impact velocity of 1070 m/s. Figure-3 demonstrates the velocities of the contact surface between the ceramic sample and the lithium fluoride window for various initial impact velocities (curve 1 corresponds to the initial impact velocity υ_0 = 544 m/s; 2 - υ_0 = 1070 m/s; 3 - υ_0 = 1573 m/s; 4 - υ_0 = 2329 m/s). For comparison, the experimental curves are given in Figure-3 [15]. The computed velocity profiles of the contact surface between the ceramic sample and the window of lithium fluoride are in good qualitative and quantitative agreement with the experimental data.

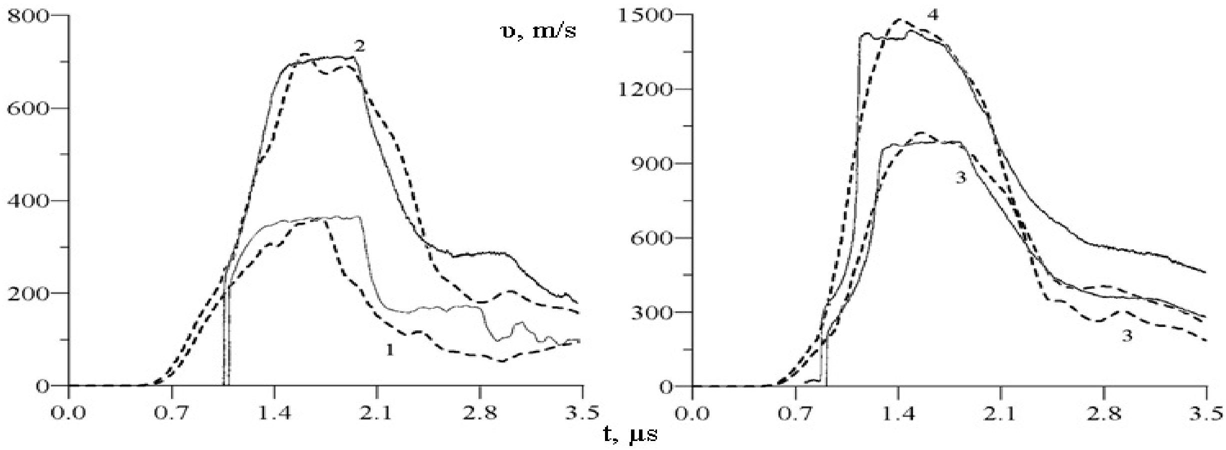

Figure-3. Rear surface velocities of the ceramic target for different loading velocities (curve 1 corresponds to the impact velocity υ_0 = 544 m/s; 2 - υ_0 = 1070 m/s; 3 - υ_0 = 1573 m/s; 4 - υ_0 = 2329 m/s). The solid lines correspond to the experiment [15], the dashed lines correspond to the computation.

EVALUATION WITH MIL COMPOSITE IMPACT TESTS

There are no experimental data on the shock compression profiles for Al_3Ti intermetallic compounds in the scientific literature. The brittle fracture model for the intermetallic material can be evaluated by comparing the computed results with the data obtained from metallic-intermetallic laminate composite impact tests.

In the experiments the Al_3Ti – Ti samples were tested using a ballistic stand and the features of the sample failure were investigated [13]. In this paper it is considered the problem concerning the interaction of a cylindrical projectile with a multilayered target consisting of seventeen composite layers (intermetallic Al_3Ti – Ti). The brittle fracture model proposed above is used to describe the fracture of the intermetallic layer in the MIL composite. Figure-4 shows the computer images with the projectile and the composite target at the time of 60 μs.

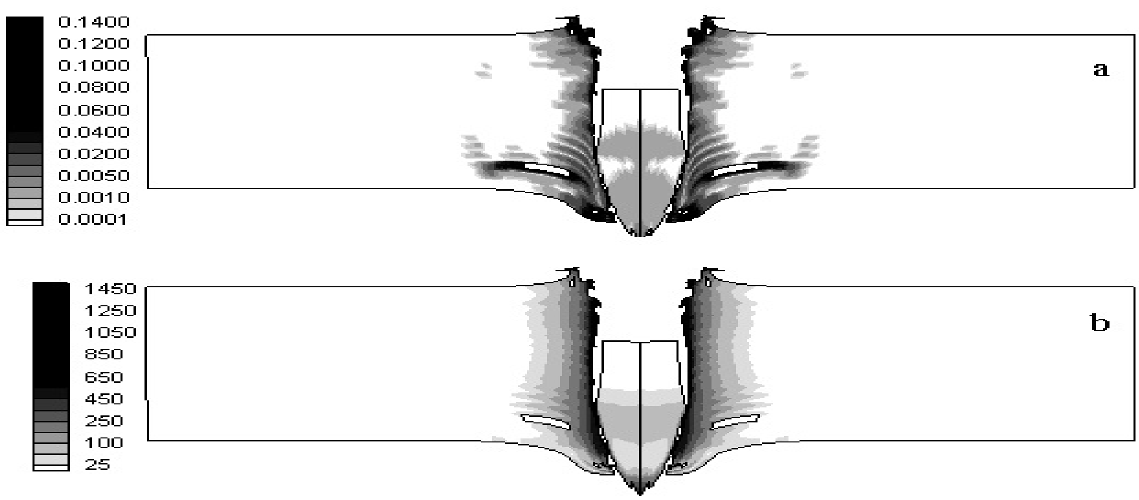

Figure-4. Configurations of the projectile, the composite target, the contours of the specific volume of microdamages V_f (cm^3/g) (a) and the specific energy of shear deformations E_{sh} (kJ/kg) (b) at the time of 60 μs.

Total thickness of the composite target was 19.89 mm. The thicknesses of the intermetallic layer and the layer of the titanium alloy were varied. The projectile used was a 93W-7FeCo tungsten heavy alloy rod with an initial diameter of 6.15 mm and a length of 23 mm. The initial impact velocity was 900 m/s. The sliding frictionless conditions are realized on the contact surfaces between the projectile and the target, and the adhesion conditions are met between the layers of the target.

The thickness of the Al_3Ti intermetallic layer in this case was 1.04 mm, the thickness of the titanium layer was 0.13 mm. Figure-4 shows the configurations of the projectile and composite target, the contours of the specific volume of microdamages and the specific energy of shear deformations. The low level of microdamages in the titanium layers shows the termination of brittle fracture in intermetallic layers.

The computations demonstrate the fact that the MIL composite target withstands the impact loading. Results of computations are in good qualitative and quantitative agreement with the experimental data [13].

CONCLUSIONS

The computational brittle fracture model was presented for the materials subjected to high velocity impact. The verification of the model was conducted using the data obtained from shock compression tests. This model was applied for dynamic loading of the Al_3Ti - Ti metallic-intermetallic laminate composite.

ACKNOWLEDGEMENTS

This work was supported by the Russian Science Foundation (RSF), project no. 16-19-10264.

REFERENCES

[1] Samsudin A.H., A.K. Hussain and J. Mahmud. 2015. Deformation and failure analysis of symmetric and antisymmetric graphite/epoxy laminate due to variations in fiber orientation. ARPN Journal of Engineering and Applied Sciences. 10(17): 7336-7344.

[2] Jayakumar T. and K. Annamalai. 2016. Mechanical behavior of modified Al-Si-Cu-Mg alloy and reinforced with Sic under ambient to elevated temperature. ARPN Journal of Engineering and Applied Sciences. 11(7): 4471-4477.

[3] D.E. Grady. 1998. Shock-wave compression of brittle solids. Mechanics of Materials. 29(3-4): 181-203.

[4] Rumyantsev B.V. 2015. Collective penetration of cumulative jets into brittle materials. Technical Physics. 60 (4): 614-617.

[5] Gorelskii V.A., S.A. Zelepugin and V.F. Tolkachev. 2000. Experimental and numerical study of ceramics destruction by high-velocity impact. Chemical Physics Reports. 18(10-11): 2211-2217.

[6] Branicio P.S., R.K. Kalia, A. Nakano, P. Vashishta, F. Shimojo and J.P. Rino. 2008. Atomistic damage mechanisms during hypervelocity projectile impact on AlN: A large-scale parallel molecular dynamics simulation study. Journal of the Mechanics and Physics of Solids. 56(5): 1955-1988.

[7] Ashby M.F. and C.G. Sammis. 1990. The damage mechanics of brittle solids in compression. Pure and Applied Geophysics. 133(3): 489-521.

[8] Kanel' G.I., S.V. Razorenov, A.V. Utkin and V.E. Fortov. 1996. Shock-Wave Phenomena in Condensed Matter. Moscow: Yanus-K.

[9] Fronczek D.M., J. Wojewoda-Budka, R. Chulist, A. Sypien, A. Korneva, Z. Szulc, N. Schell, P. Zieba. 2016. Structural properties of Ti/Al clads manufactured by explosive welding and annealing. Materials and Design. 91: 80–89.

[10] K.S. Vecchio. 2005. Synthetic multifunctional metallic-intermetallic laminate composites. JOM. 57(3): 25-31.

[11] Patselov A., B. Greenberg, S. Gladkovskii, R. Lavrikov and E. Borodin. 2012. Layered metal-intermetallic composites in Ti-Al system: strength under static and dynamic load. AASRI Procedia. 3: 107-112.

[12] Zelepugin S.A., V.I. Mali, A.S. Zelepugin and E.V. Ilina. 2012. Failure of metallic-intermetallic laminate composites under dynamic loading. AIP Conference Proceedings. 1426: 1101-1104.

[13] Zelepugin S.A. and A.S. Zelepugin. 2014. Failure of multilayer composites under dynamic loading. 11th World Congress on Computational Mechanics, WCCM 2014, 5th European Conference on Computational Mechanics, ECCM 2014 and 6th European Conference on Computational Fluid Dynamics, ECFD 2014. 4: 3926-3933.

[14] Cao Y., S. Zhu, C. Guo, K.S Vecchio and F. Jiang. 2015. Numerical investigation of the ballistic performance of metal-intermetallic laminate composites. Applied Composite Materials. 22(4): 437-456.

[15] Grady D.E. and R.L. Moody. 1996. Shock compression profiles in ceramics. Sandia National Laboratories Technical Report, SAND96-0551.

[16] Johnson G.R. 2011. Numerical algorithms and material models for high-velocity impact

computations. International Journal of Impact Engineering. 38(6): 456-472.

[17] Gorelski V.A., S.A. Zelepugin and A.Yu. Smolin. 1997. Effect of discretization in calculating three-dimensional problems of high-velocity impact by the finite-element method. Computational Mathematics and Mathematical Physics. 37(6): 722-730.

[18] Gust W.H. and E.B. Royce. 1971. Dynamic yield strengths of B_4C, BeO and Al_2O_3 ceramics. Journal of Applied Physics. 42(1): 276-295.